Temperature Dependence of Ag Film Roughening during Deposition on Quasicrystal and Approximant Surfaces

B. Ünal[a,b,†], J.W. Evans[a,c] and P.A. Thiel[a,b,d,*]

[a]The Ames Laboratory, [b]Department of Materials Science and Engineering, [c]Department of Physics and Astronomy, and [d]Department of Chemistry, Iowa State University, Ames, Iowa 50011, USA

The temperature (T) dependence of roughening as assessed by scanning tunneling microscopy is compared for growth of Ag films on an 5-fold icosahedral Al–Pd–Mn quasicrystal surface and on an ξ'-approximant. Growth on the quasicrystal corresponds to a version of the Volmer–Weber growth, but modified by quantum size effects, and also by kinetic smoothening at low T and low coverages (θ). Growth on the approximant corresponds to a version of the Stranski–Krastanov growth modified by kinetic roughening at low T and low θ. For larger θ, i.e., for thicker films, distinct behavior is observed.

1. Introduction

Using quasicrystals and other complex intermetallics/ alloys, as substrates for metallic film growth, has led to several intriguing discoveries [1, 2]. These include: (i) pseudomorphism, in which the metallic overlayer mimics the geometric structure of the substrate, (ii) non- -standard nucleation phenomena, in which specific ad- sorption sites on the substrate act as traps, resulting in a combination of heterogeneous and homogeneous nu- cleation characteristics, and (iii) a quantum size effect, in which the Fermi wavelength-matching of electrons within films or islands stabilizes particular thicknesses or heights. Noble metals are particularly useful for reveal- ing such new phenomena, since their driving force for alloying with other metals is usually low. The goal of the present work is to explore and compare the growth modes of metallic films on quasicrystal and related substrates, specifically assessing the temperature-dependence of the development of film roughness. We choose Ag as the film material because in past studies, there has been no evidence for intermixing within the temperature range examined here [3], nor would intermixing be expected in this regime based on published work for other systems.

First, we review the classic thermodynamic picture for epitaxial thin film growth modes [4]. When a film is *equilibrated*, and when intermixing (alloying) does not occur, there are two extrema in the way that film mor- phology develops with coverage, θ. The first is two- -dimensional (2D), or layer-by-layer (LBL) growth, also called the Frank–van der Merwe (FvdM) growth. This occurs when the surface energy of the adsorbed mate- rial is less than or equal to its adhesion energy with the substrate. It *always* applies in homoepitaxy, and

it *often* applies in situations where a low-surface-energy material is deposited on a high-surface-energy substrate. At the other extreme is three-dimensional (3D) or the Vollmer−Weber (VW) growth, wherein the film reduces interfacial area by forming 3D islands or clumps. This occurs when the surface energy of the adsorbed material is greater than its adhesion energy with the substrate, and it often applies when a high-surface-energy material is deposited on a low-surface-energy substrate. A third Stranski–Krastanov (SK) growth mode can be considered as intermediate, since there the film grows layer-by-layer for the first one or few layers, then changes to 3D growth because cumulative strain buildup for thicker films re- duces the adhesion energy.

In fact, deposition drives the system out of equilib- rium, and the growth morphology can be quite far-from- -equilibrium especially at lower temperatures (T) due to kinetic limitations [5, 6]. Thus, the T-dependence pro- vides useful insight, because one expects that the equili- brated structure is revealed at higher deposition T. For 2D FvdM growth, inhibited downward interlayer trans- port at low T leads to the kinetically-limited film be- ing rougher than in equilibrium. Actual behavior can be more complex (including reentrant smooth growth for very low T) as described in the next subsection [7, 8]. For 3D VW growth, inhibited upward interlayer trans- port at low T leads to smoother growth. We call these non-equilibrium effects kinetic roughening [5, 6] and ki- netic smoothening, respectively.

Finally, we remark that other growth modes are pos- sible which are relevant for the systems of interest here. Specifically, growth influenced by quantum size effects (QSE) can result in development of multilayer mesa-like islands with selected or "magic" heights [9], even in metal- -on-metal films [10]. Thus, one could imagine a type of quasi-layer-by-layer growth (at least up to one complete quasi-layer), but where the quasi-layers have the selected multilayer height.

In Sect. 2, we define film roughness, W, as a way to quantify and compare the behavior described above for

———

corresponding author; e-mail: pthiel@iastate.edu

[†]Present address: Department of Chemical Engineering, MIT, U.S.A.

different growth modes. This behavior of W versus coverage, θ, is shown schematically for various cases. In Sect. 3, we present experimental data from scanning tunneling microscopy (STM) studies for the T-dependence of the growth of Ag films on the 5-fold surface of the icosahedral Al–Pd–Mn quasicrystal and on a so-called ξ'-approximant of the Al–Pd–Mn quasicrystal. These observations are interpreted in the context of the different growth modes discussed above and in Sect. 2. Conclusions and further discussion are presented in Sect. 4.

2. Film roughness

Roughness is the key parameter for characterizing film growth modes. The root-mean-square roughness, W, is defined as the root-mean-square of the deviation of the film height, $h = h(\boldsymbol{x}, t)$, at lateral position $\boldsymbol{x}$ and time t, from its average, $\langle h \rangle$, over lateral position [5, 6]. For a film with well-defined layers and fixed interlayer spacing, b, it is convenient to introduce a normalized discrete film height distribution, P_j, which gives the fraction of the surface with height $h = bj$. Then, the average height satisfies $\langle h \rangle = b\langle j \rangle = b\sum_{j\geq 0} jP_j$. The standard scenario of relevance here is deposition at constant rate F monolayers (ML) per unit time on a surface starting at $h = 0$ for $t = 0$, so that $\langle j \rangle = Ft = \theta$. The film roughness, W, satisfies [5, 6]:

$$W^2 = \langle (h - \langle h \rangle)^2 \rangle = b^2 \sum_{j\geq 0} (j - \langle j \rangle)^2 P_j. \tag{1}$$

Next, we describe the variation of W as a function θ for the various thermodynamic growth modes described in Sect. 1, as well as non-equilibrium deviations typically seen for lower T [5, 6]. This behavior is shown schematically in Fig. 1. First, we consider thermodynamic FvDM or LBL growth systems. For initial growth of the first layer with $0 \leq \theta \leq 1$, one has $P_0 = 1 - \theta$ and $P_1 = \theta$, so that

$$W^2 = b^2\theta(1 - \theta), \quad \text{for} \quad 0 \leq \theta \leq 1 \quad \text{(FvDM)}, \tag{2}$$

and this behavior repeats with periodicity of 1 ML. Next, we describe non-equilibrium kinetic roughening. The traditional picture is that as T is lowered, inhibited downward transport (often due to an additional Ehrlich–Schwoebel step edge barrier) leads to a monotonic increase in W saturating at $W^2 = b^2\theta$. This value corresponds to the Poisson growth, $P_j = \exp(-\theta)\theta^j/j!$, reflecting a complete lack of interlayer transport (but possible intralayer transport). This type of behavior is seen for Ag film growth on Ag(111) surfaces [6] (although ideal Poisson growth is not achieved). In fact, the Poisson growth is typically associated with a simple solid-on-solid simple-cubic (sc) crystal model for growth at $T = 0$ K in the complete absence of surface diffusion, where deposited atoms hit-and-stick even on top of isolated adatoms.

Actually, this picture is too simplistic for any realistic crystalline (e.g., fcc or bcc) structure, or even quasicrystalline film structure. Deposited atoms tend to
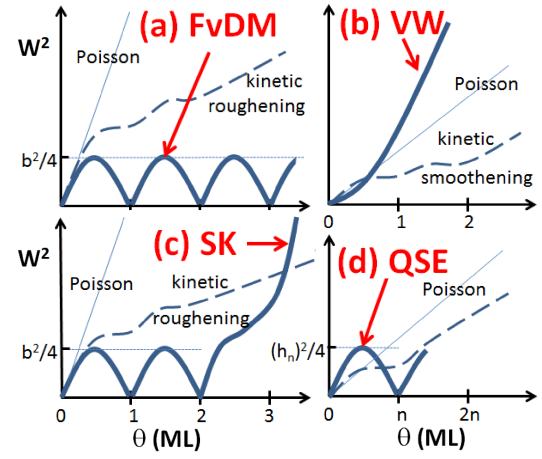

Fig. 1. Schematic of the behavior of mean-square roughness, W, versus coverage θ. Classic behavior for (a) FvDM, (b) VW, (c) SK, (d) QSE growth modes is shown as thick solid curves. Also shown in non-equilibrium deviations (kinetic roughening or smoothening) and also Poisson growth.

"funnel downward" from isolated adatoms and step edges to lower adsorption sites [11]. The population of such steps increases greatly at low T due to a reduction in the lateral correlation length or typical lateral feature size. This would actually produce smooth Edwards–Wilkinson growth with $W^2 \sim \ln\theta$ at low T [12]. Thus, a more realistic picture of the T-dependence of growth for FvDM systems is that one goes from LBL growth at higher T to rougher growth with kinetic roughening with $W^2 \sim \theta^{2\beta}$ and $\beta \approx 1/4$ to $1/3$ at moderate T, to possibly smoother growth at low T due to downward funneling [5, 6]. (One caveat is that typical experimental data does not sample true asymptotic β-values.) Thus, for fixed θ, it is reasonable to expect a non-monotonic variation from smooth growth at high T to rougher growth at moderate T to "reentrant" smooth growth at low T [7, 8]. Of some relevance here, this behavior is clearly apparent in growth of Ag films on Ag(100) surfaces [13–15].

Second, consider thermodynamic VW growth systems involving the immediate development of 3D islands. It is reasonable to expect that these have a fixed equilibrium shape determined by a competition between film surface and adhesion energies. For a simple analysis, suppose that the typical separation, L_{isl}, between islands is roughly constant except for very low coverage (i.e., most island nucleation occurs very early). Then, if R denotes a typical island radius, one has that the volume of islands scales like $R^3 \sim b\theta(L_{\text{isl}})^2$. In the regime where only a small fraction, $\theta_{2\text{D}} \sim (R/L_{\text{isl}})^2$, of the substrate is covered by the footprint of 3D islands, one estimates that

$$W^2 \sim R^2\theta_{2\text{D}}(1 - \theta_{2\text{D}}) \sim R^2\theta_{2\text{D}}$$

$$\sim b^{4/3}(L_{\text{isl}})^{2/3}\theta^{4/3} \quad \text{(VW)}. \tag{3}$$

With regard to non-equilibrium kinetic smoothening, one anticipates that restricted upward transport for lower T

inhibits formation of equilibrated 3D island shapes, and thus leads to smoother films. For very low T, downward funneling should play a significant role inducing smoother film growth.

Third, for thermodynamic SK growth, behavior of W versus θ can be deduced from the above discussion. Specifically, one expects initial FvDM behavior as in (2) or non-equilibrium deviations thereof. Above a critical coverage, θ_c, for 3D island formation, one expects VW--type behavior, i.e., $W^2 \sim b^{4/3}(L_{isl})^{2/3}(\theta - \theta_c)^{4/3}$.

Fourth, for a quasi-layer-by-layer QSE growth mode with n-layer islands or mesas with selected height, h_n, a simple adaptation of the FvDM result shows that [16]:

$$W^2 \approx (h_n)^2(\theta/n)[1 - (\theta/n)],$$

$$\text{for} \quad 0 \leq \theta \leq n \quad \text{(QSE)}. \tag{4}$$

Finally, we comment on some complications to the above picture for the systems of interest here. First, we note that the FvDM result (2) is implicitly based on a picture of "sharp steps" between layers so the film height is either $h = 0$ or $h = b$. In fact, the STM tip smears step edges so the effective measured $h(\boldsymbol{x})$ varies continuously across step edges. This effect is generally not significant at higher T, but can result in a significant reduction of W (relative to the FvDM value) in the lower T regime with a high density of step edges. As a simple example, consider a FvDM film morphology for $\theta = 1/2$ ML with equal--sized periodically-located 2D square islands with center separation L_{isl}. Then if the tip smears linear steps to linear profiles varying between $h = 0$ and $h = b$ over a distance rL_{isl} with $r \leq 1/2$ (and one neglects possibly distinct behavior at island corners), one finds that

$$W^2 = (1 - 4r/3)b^2/4, \quad \text{at} \quad \theta = \frac{1}{2} \text{ ML}$$

$$\text{(FvDM + tip smearing)}, \tag{5}$$

which is reduced from the classic FvDM value corresponding to $r = 0$. (The minimum value $W^2 = b^2/12$ for $r = 1/2$ corresponds to that for a simple saw-tooth height profile.) Second, we mention that the assumption of a layer or height independent interlayer spacing, b, is actually an oversimplification for the systems of interest here where the first few layers actually tend to have different, varying interlayer spacing [16]. In this situation, it is more appropriate to use a dimensionless roughness, w, satisfying $w^2 = \sum_{j \geq 0}(j - \langle j \rangle)^2 P_j$. However, we neglect this complication in the current study.

3. Experimental observations: Ag/Al–Pd–Mn QC and Ag/ξ′-approximant

Experimental conditions have been described elsewhere [16, 17]. Briefly, the experiments are carried out with an Omicron variable-temperature scanning tunneling microscope (STM) in ultrahigh vacuum. Ag is deposited via physical vapor deposition with the substrate held at a temperature T. More details of the substrates can also be found in Ref. [17]. The deposition flux used here is $F \approx 10^{-3}$ ML/s. The STM images are taken at

the deposition temperature. STM data are processed using image processing freeware [18]. Using this software, the RMS values are calculated from 100 nm × 100 nm images. Each RMS value is obtained from a single terrace.

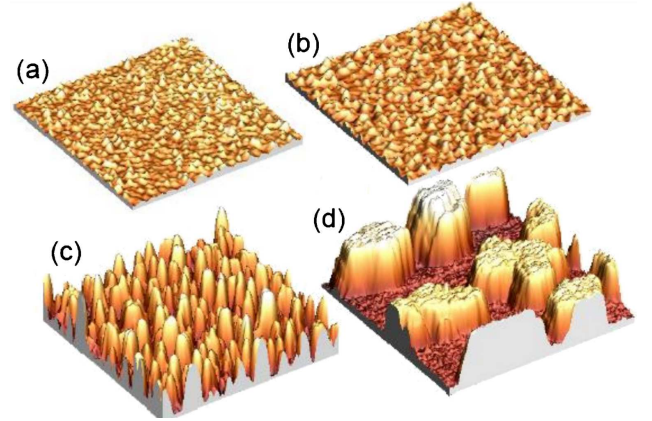Fig. 2. Topographic STM images (100 nm × 100 nm) of Ag on 5-fold icosahedral Al–Pd–Mn, at ≈ 1 ML Ag coverage. The deposition temperatures are (a) 130 K, (b) 200 K, (c) 300 K and (d) 365 K.

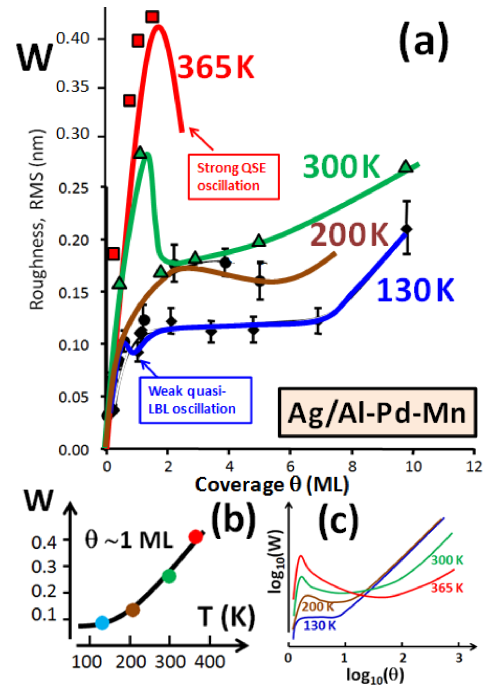Fig. 3. Deposition of Ag on 5-fold icosahedral Al–Pd–Mn. (a) Film roughness, W, versus coverage, θ, for $T = 130, 200, 300,$ and 365 K. (b) W versus T for $\theta \approx 1$ ML. (c) Speculated behavior of W for larger θ (thicker films) for various T.

Figures 2 and 3 illustrate the variation of film morphology for Ag on a 5-fold icosahedral Al–Pd–Mn quasicrystal surface at four different values of $T = 130, 200, 300,$ and 365 K. Figure 3 shows the STM data in semi-three--dimensional representation. Figure 3a gives roughness,

W, as a function of θ. Figure 3b shows the variation of W with T at $\theta \approx 1$ ML. The form of W versus T clearly indicates behavior associated with VW-type growth systems, since W is an increasing function of T over the range 130 K to 365 K. The variation of $W(\theta)$ with θ at lowest growth temperature, 130 K, also shows a small dip (weak oscillation) at about 1 monolayer (ML), as expected for strong kinetic smoothening and initial quasi-LBL growth at sufficiently low T.

In fact, we claim that behavior in this system corresponds to a QSE growth mode. Specifically, growth at 365 K is mediated by a quantum size effect that strongly favors three-layer-high islands of Ag [16, 19]. The kinetics of island formation in this regime have been modeled in detail [16]. In Fig. 3a, the curve drawn nearly through the $W(\theta)$ data points at 365 K is the prediction of a simple analytic model in which roughness is given by (4) with $n = 3$ and $h_3 \approx 0.82$ nm (as determined from experiment). This model fits the experimental roughness at 365 K quite well, although we do not have data for W above 1.4 ML to directly confirm the proposed strong dip in W above 1.5 ML. However, experimental behavior at 300 K where QSE growth is rather imperfect shows an analogous dip. This provides support for our claim of a dip at 365 K.

It is instructive to comment on anticipated behavior for higher coverages. Previous studies of the growth of thicker Ag films indicate a tendency for these films to transform to a fcc(111) structure [19]. Thus, homoepitaxial growth on Ag(111) (FvDM systems) provides a reasonable paradigm for growth of such thicker films. From this perspective, one expects asymptotically Poisson-like growth with $W^2 \approx 0.21b^2\theta$ at 200 K and below, and with $W^2 \approx 0.09b^2\theta$ at 300 K, but significantly smoother growth with $W^2 \approx 0.07b^2\theta^{0.72}$ at the highest $T = 365$ K, and where $b = 0.236$ nm for Ag(111). These results come from analysis of Ag/Ag(111) homoepitaxy [20] using interpolation to assess behavior at 365 K. A schematic of expected behavior is shown in Fig. 2c. (One caveat is that actually the film displays multiple mis-oriented fcc(111) domains, each epitaxially related to the 5-fold icosahedral substrate [17]. This feature will no doubt perturb W behavior from that in Ag(111) homoepitaxy.)

Figure 4 illustrates the variation of roughness, W, with θ for Ag on the pseudo-tenfold surface of the ξ'-approximant Al–Pd–Mn surface at three different values of $T = 130$, 200, and 300 K. The form of $W(\theta)$ suggests behavior associated with SK-type growth systems, since W versus θ remains low at the highest $T = 300$ K up to an apparent $\theta_c \approx 6$–8 ML, after which W increases strongly with θ consistent with the simple form proposed in Sect. 2 for SK growth. For lower $T = 130$ K and 200 K, W is generally larger than at 300 K for a range of lower θ up to about 6 ML consistent with kinetic roughening. In fact for $\theta \approx 2$–4 ML, W versus T is non-monotonic, consistent with re-entrant smooth growth at the lowest $T = 130$ K (see Fig. 4, inset).
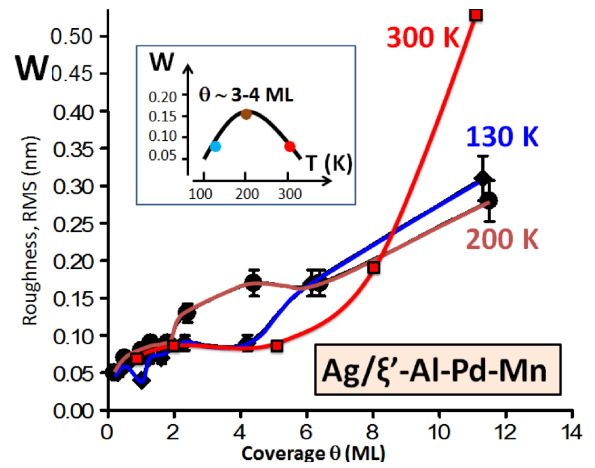

Fig. 4. Deposition of Ag on the ξ'-approximant: film roughness, W, versus coverage, θ, for $T = 130$, 200, and 300 K. Inset: W versus T for $\theta \approx 3$–4 ML.

As for deposition on the quasicrystal described above, the variation of $W(\theta)$ at lowest growth temperature, 130 K, also shows a small dip (weak oscillation) at about 1 monolayer (ML). However, the maximum value of W of 0.06 nm up to 1 ML at 130 K appears slightly below the LBL value b/2 with $b = 0.142$ nm for the first layer. This is presumably a consequence of tip smearing discussed in Sect. 2. (One caveat with the above analysis is that the interlayer spacing varies significantly for the first few layers, and also varies with T. However, correcting for this variation still reveals re-entrant smooth growth at 130 K.) For larger coverages above $\theta \approx 8$ ML, growth at lower T is smoother than that associated with SK growth at 300 K, this behavior corresponding to kinetic smoothening.

4. Discussion and conclusions

Using traditional concepts of thermodynamic film growth modes dating back to the late 1950's [4], as well as the detailed understanding of non-equilibrium growth due to kinetic limitations developed during the last two decades [5, 6], we are able to provide a detailed characterization and elucidation of Ag film growth on the 5-fold Al–Pd–Mn quasicrystal surface, as well as on a ξ'-approximant. One finds QSE–VW type behavior for the former, and SK type behavior for the latter. This difference can reflect different surface energies for the two substrates, different degrees of epitaxial match between film and substrate, and strong QSE for the Al–Pd–Mn quasicrystal surface. For completeness, we briefly comment on another study of Ag film growth on a decagonal Al–Cu–Co quasicrystal [21]. Interestingly, this surface exposes two distinct types of terraces: one is an Al-rich termination, and the other a transition metal (TM) rich termination. Adhesion of the Ag film to the Al-rich termination is weaker than to the Al-rich termination. As a result, one finds rougher growth on the former and

smoother growth on the latter. Furthermore at 5 ML, one finds that film roughness decreases monotonically with decreasing T for the Al-rich termination (as for the Ag on Al–Pd–Mn quasicrystal), and reentrant smooth growth for the TM-rich termination (as for Ag on the ξ'-approximant) [21].

Acknowledgments

References

[1] V. Fournée, P.A. Thiel, *J. Phys. D, Appl. Phys.* **38**, R83 (2005).

[2] V. Fournée, J. Ledieu, M. Shimoda, M. Krajčí, H.-R. Sharma, R. McGrath, *Isr. J. Chem.* **51**, 1314 (2011).

[3] B. Ünal, F. Qin, Y. Han, D.J. Liu, D. Jing, A.R. Layson, C. Jenks, J.W. Evans, P.A. Thiel, *Phys. Rev. B* **76**, 195410 (2007).

[4] E. Bauer, *Z. Kristallogr.* **110**, 372 (1958); **110**, 395 (1958).

[5] T. Michely, J. Krug, *Islands, Mounds, and Atoms: Patterns and Processes in Crystal Growth Far-from-Equilibrium*, Springer, Berlin 2004.

[6] J.W. Evans, P.A. Thiel, M.C. Bartelt, *Surf. Sci. Rep.* **61**, 1 (2006).

[7] R. Kunkel, B. Poelsema, L.K. Verheij, G. Comsa, *Phys. Rev. Lett.* **65**, 733 (1990).

[8] M.C. Bartelt, J.W. Evans, *Surf. Sci.* **423**, 189 (1999).

[9] A.R. Smith, K.-J. Chao, Q. Niu, C.-K. Shih, *Science* **273**, 226 (1996).

[10] Y. Han, B. Unal, D. Jing, P.A. Thiel, J.W. Evans, D.-J. Liu, *Materials* **3**, 3965 (2010).

[11] J.W. Evans, D.E. Sanders, P.A. Thiel, A.E. DePristo, *Phys. Rev. B (Rapid Commun.)* **41**, 5410 (1990).

[12] H.C. Kang, J.W. Evans, *Surf. Sci.* **269-270**, 784 (1992).

[13] C.R. Stoldt, K.J. Caspersen, M.C. Bartelt, C.J. Jenks, J.W. Evans, P.A. Thiel, *Phys. Rev. Lett.* **85**, 800 (2000).

[14] G. Constantini, F. Buatierde Mongeot, C. Boragno, U. Valbusa, *Surf. Sci.* **459**, L487 (2000).

[15] K.J. Caspersen, C.R. Stoldt, A.R. Layson, M.C. Bartelt, P.A. Thiel, J.W. Evans, *Phys. Rev. B* **63**, 085401 (2001).

[16] B. Ünal, V. Fournée, P.A. Thiel, J.W. Evans, *Phys. Rev. Lett.* **102**, 196103 (2009).

[17] V. Fournée, A.R. Ross, T.A. Lograsso, J.W. Evans, P.A. Thiel, *Surf. Sci.* **537**, 5 (2003).

[18] I. Horcas, R. Fenández, J.M. Gómez-Rodriguez, J. Colchero, J. Gómez-Herrero, A.M. Baro, *Rev. Sci. Instrum.* **78**, 013705 (2007).

[19] V. Fournée, H.R. Sharma, M. Shimoda, A.P. Tsai, B. Unal, A.R. Ross, T.A. Lograsso, P.A. Thiel, *Phys. Rev. Lett.* **95**, 155504 (2005).

[20] W.C. Elliott, P.F. Miceli, T. Tse, P.W. Stephens, *Phys. Rev. B* **54**, 17938 (1996).

[21] T. Duguet, B. Unal, Y. Han, J.W. Evans, J. Ledieu, C.J. Jenks, J.M. Dubois, V. Fournee, P.A. Thiel, *Phys. Rev. B* **82**, 224204 (2010).